Macromolecules

Cite This: Macromolecules 2018, 51, 8316–8323

Article

pubs.acs.org/Macromolecules

Rapid and Quantitative De-*tert*-butylation for Poly(acrylic acid) Block Copolymers and Influence on Relaxation of Thermoassociated Transient Networks

Alexei D. Filippov,[†] Ilse A. van Hees,[†] Remco Fokkink,[†] Ilja K. Voets,[‡] and Marleen Kamperman*[,†,§]

[†]Laboratory of Physical Chemistry and Soft Matter, Wageningen University & Research, Stippeneng 4, 6708WE Wageningen, The Netherlands

[‡]Institute for Complex Molecular Systems, Eindhoven University of Technology, P.O. Box 513, 5600 MB Eindhoven, The Netherlands

[§]Zernike Institute of Advanced Materials, University of Groningen, 9747 AG Groningen, The Netherlands

Supporting Information

ABSTRACT: The synthesis of charged polymers often requires the polymerization of protected monomers, followed by a polymer-analogous reaction to the polyelectrolyte product. We present a mild, facile method to cleave *tert*-butyl groups from poly(*tert*-butyl acrylate) blocks that yields poly(acrylic acid) (pAA) blocks free of traces of the ester. The reaction utilizes a slight excess of HCl in hexafluoroisopropanol (HFIP) at room temperature and runs to completion within 4 h. We compare deprotection in HFIP with the common TFA/DCM method and show that the latter does not yield clean pAA. We show the effect of complete *tert*-butyl cleavage on a ABA triblock copolymer, where poly(*N*-isopropylacrylamide) (pNIPAM) is A and pAA is B, by means of viscosimetry, DLS, and SAXS on solutions above overlap. The pNIPAM blocks dehydrate, and their increased self-affinity above the lower critical solution temperature (LCST) results in network formation by the triblocks. This manifests itself as an increase in viscosity and a slowing down of the first-order correlation function in light scattering. However, this stickering effect manifests itself exclusively when the pAA block is *tert*-butyl-free. Additionally, SAXS shows that the conformational properties of *tert*-butyl-free pAA copolymers are markedly different from those with residual esters. Thus, we illustrate a surprising effect of hydrophobic impurities that act across blocks and assert the usefulness of HCl/HFIP in pAA synthesis.

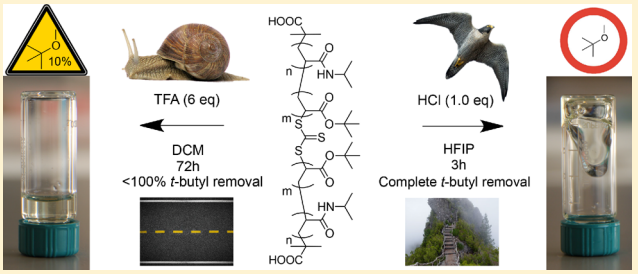

INTRODUCTION

Acrylic acid (AA) is the smallest unsaturated carboxylic acid and can be polymerized radically. By virtue of the carboxylic moiety, the resulting polymers are polyelectrolytes and have a pH-dependent charge and H-bonding capacity. In copolymers, AA is used to tailor responsive behavior of other polymeric building blocks, such as the swelling of hydrogels[1,2] and the lower critical solution temperature (LCST) of poly(*N*-isopropylacrylamide) (pNIPAm) and its copolymers.[3] pAA is one of the most studied polyanions in polyelectrolyte complexes, owing to its ability to form complexes with many polycations.[4,5]

In radical polymerizations, acrylic acid is unusually inclined to transfer reactions to solvent,[6] transfer to polymer,[7] and formation of Michael dimers.[8] These side reactions result in diminished control over linearity, molecular weight distribution, and end-group fidelity of the polymer products.[8,9] There are many reports that detail pAA synthesis with the help of controlled radical polymerization (CRP) techniques, in particular reversible addition−fragmentation chain transfer (RAFT).[6,10,11] Chain transfer agents are known to reduce branching and termination by ensuring a low concentration of active radicals.[7] Nonetheless, it is difficult to prepare strictly linear polymers directly from AA due to its high rate and extensive repertoire of side reactions, and branching is often overlooked in reports on pAA.[6,8] Given the difficulties of direct polymerization of AA, pAA is often made in a two-step process starting from a precursor monomer that is less affected by transfer reactions, followed by a polymer-analogous reaction that yields pAA.

A canonical two-step method relies on the ester of acrylic acid and *tert*-butanol, the latter acting analogously to a protecting group. *tert*-Butyl acrylate (*t*BuAc) can be polymerized by anionic or radical means, and the resulting polymer is de-esterified into pAA under acidic conditions, trifluoroacetic acid in DCM (TFA/DCM) being especially common.[12−17] However, even a strong molar excess yields pAA with at most 99.5% liberated carboxylic acid, the rest being still

Received: July 6, 2018
Revised: September 19, 2018
Published: October 12, 2018

DOI: 10.1021/acs.macromol.8b01440
Macromolecules 2018, 51, 8316–8323

esterified with *tert*-butanol.[6,14] The incomplete cleavage remains unaddressed, even though residual *tert*-butyl groups can affect polymer properties. Foreseeable effects are an increase of surface pressure at water−apolar interfaces and a greater tendency to form complexes through hydrophobic interactions, since the resulting structures are comparable to hydrophobically modified pAA. Thus, a means of obtaining ester-free pAA from p*t*BuAc is desirable.

In the present work, we report a cleavage reaction that yields quantitatively de-*tert*-butylated pAA rapidly, based on the work of Palladino and co-workers.[18] We apply the method to the synthesis of a triblock copolymer with a monomer that is representative[1,19] of the use of pAA in the literature, pNIPAm. Full *tert*-butyl ester cleavage is shown by NMR. To assert the necessity of complete deprotection of p*t*BuAc precursors, we show that the ubiquitous TFA/DCM conditions yield polymers with markedly distinct flow and conformational properties, as witnessed by viscosity, dynamic light scattering (DLS), and small-angle X-ray scattering measurements (SAXS).

EXPERIMENTAL SECTION

Materials. 2,2′-Azobis(2-methylpropionitrile) (AIBN, 98%), *N*-isopropylacrylamide (NIPAm, 97%), *tert*-butyl acrylate (*t*BuAc, contains 10−20 ppm monomethyl ether hydroquinone as inhibitor, 98%), trioxane (⩾99.9%), trifluoroacetic acid (TFA, ⩾99%), concentrated HCl (37% solution in water), and dioxane (anhydrous, 99.8%) were obtained from Sigma-Aldrich, Germany, and used without further purification unless noted otherwise. NIPAm was recrystallized twice from a mixture of hexane and acetone. *t*BuAc was passed over a short column of Al_2O_3 to remove the inhibitor. AIBN was recrystallized thrice from MeOH. Bis(2-methylpropionic acid)-trithiocarbonate[20,21] (BMAT) and BMAT-terminated pNIPAm[21] were synthesized as described in the literature, with NMR and SEC characterization described in Table S1. Hexafluoroisopropanol (HFIP, AR), dichloromethane (DCM, AR), tetrahydrofuran (THF, HPLC-grade), and methanol (MeOH, HPLC) were obtained from Biosolve, France.

Synthesis of pNIPAm-*b*-p*t*BuAc-*b*-pNIPAm. A Schlenk flask was charged with a solution of BMAT-terminated $pNIPAm_{24}$ (0.581 g, 0.104 mmol), *t*BuAc (5.3 g, 41.4 mmol), AIBN (3.4 mg, 0.020 mmol), and trioxane (0.372 g, 4.14 mmol) in dioxane (21 mL) and was subjected to five freeze−pump−thaw cycles. The solution was magnetically stirred at 70 °C for 45 min, after which the polymerization was stopped by admitting atmosphere into the flask while cooling on an ice bath. The material was precipitated thrice in ice-cold MeOH:water 3:1 and dried under high vacuum.

TFA/DCM Deprotection of pNIPAm-*b*-p*t*BuAc-*b*-pNIPAm. pNIPAm-*b*-p*t*BuAc-*b*-pNIPAm (1.05 g, 0.023 mmol) was dissolved in DCM (50 mL) in a round-bottomed flask, to which was added 6 equiv of TFA (4.2 g, 39 mmol) with respect to the amount of *t*Bu units. The mixture was stirred for 72 h at room temperature; the precipitated product was washed with fresh DCM and extensively dried under high vacuum. The dry polymer was dispersed in water by sonication and titrated with an NaOH solution until the solution was neutral. Water was removed by freeze-drying. This yielded pNIPAm-(pAA-*co*-p*t*BuAc)-*b*-pNIPAm as a white, fluffy powder.

HCl/HFIP Deprotection of pNIPAM-*b*-p*t*BuAc-*b*-pNIPAm. pNIPAm-*b*-p*t*BuAc-*b*-pNIPAm (3.5 g, 0.093 mmol) was dissolved in HFIP (314 mL) in a round-bottomed flask, to which concentrated HCl 37% (2.6 mL, 31.4 mmol) was added, 1.3 equiv with respect to the amount of *t*Bu units. After 4 h, the mixture was stripped of volatiles, and the dry polymer was dispersed in water and titrated with an NaOH solution until the solution was neutral. A slight cloudiness was removed by centrifugation at 15000*g*, and the supernatant was dehydrated by freeze-drying. pNIPAm-*b*-pAA-*b*-pNIPAm was recovered as a white fluffy powder.

Polymer Characterization. ^1H and ^{13}C NMR measurements were performed on a Bruker AVANCE 400 spectrometer. Fourier transform infrared absorption spectra were collected on a Bruker PLATINUM ATR mounted into a TENSOR spectrometer on powdered sample. A background was taken and subtracted from the spectra, followed by baseline correction and transformation from transmission to absorption.

Size-Exclusion Chromatography (SEC). SEC of pNIPAm and its copolymers with p*t*BuAc was done on a Agilent 1200 HPLC equipped with a PLgel 5 μm Mixed-D column with RI detection, calibrated with polystyrene standards, and HPLC-grade THF as eluent. The presence of pNIPAm blocks complicates the analyses due to column−analyte interactions. The problem is somewhat remedied in an aqueous SEC system on corresponding de-*tert*-butylated products. Aqueous size exclusion chromatography of pAA copolymers was done in an aqueous buffer of 0.01 M Na_2HPO_4/NaH_2PO_4 with 0.1 M $NaNO_3$ on an Agilent 1260 Infinity II HPLC equipped with a Waters Ultrahydrogel 500 column for molecular weight analysis. Analytes were detected with a refractive index detector and by UV adsorption.

Trithiocarbonate Cleavage with Hydrazine. In adaptation of a previous report,[22] the sodium salt of BMAT-derived triblock pNIPAm-*b*-pAA-*b*-pNIPAm (0.100 g, 3.34 μmol of trithiocarbonates) was dissolved in water (11 mL), to which was added 5 equiv of hydrazine (1 μL, 16.7 μmol). The mixture was stirred at room temperature for 72 h, and an aliquot was diluted 1:3 with 0.01 M Na_2HPO_4/NaH_2PO_4 with 0.1 M $NaNO_3$, which was analyzed with SEC over an Agilent PL AquaGel-OH 8 μm column and compared with an aliquot of nontreated sample.

DLS of Triblock Solutions. DLS measurements on triblock networks were performed in the manner described by Bohdan et al.[23] An ALV light scattering apparatus equipped with a 632.8 nm JDSU 1145P laser and a LSE-5004 correlator was used. Temperature was controlled by means of a Julabo water bath. DLS measures the electric field autocorrelation function $g_2(t) = \langle I(0)I(t)\rangle/\langle I^2\rangle$ from which the normalized first-order correlation function $g_1(t)$ is obtained:

$$g_1(t) = \beta^{-1/2}\sqrt{g_2(t) - 1} \tag{1}$$

in which β is a geometry-dependent constant close to unity. We describe $g_1(t)$ by a two-mode stretched exponential decay:

$$g_1(t) = \sum_{i=f,s} A_i \exp\left(-\frac{t_i^{\alpha}}{\tau_i}\right) \tag{2}$$

where τ is the exponential decay time and α is the stretch parameter. The latter characterizes the width of the decay time distribution, with $\alpha_i = 1$ corresponding to a simple exponential decay and smaller values to a more stretched shape, and thus a broader decay time distribution. The subscripts f and s refer to respectively the fast and slow modes that we observe for all relaxations.[24]

Samples were made by addition of 1 mL water to 292 mg of polymer and were filtrated over 0.2 μm regenerated cellulose (RC) syringe filters after dissolution. Correlation curves were recorded for times between 3000 and 10000 s to ensure full decay of $g_1(t)$, with higher temperatures resulting in slower decays.

Rheology of Triblock Solutions. Rheological measurements were recorded on an Anton Paar MCR-301, using a 1 mL Couette geometry and temperature control by a Peltier system. Evaporation was avoided by the use of a tetradecane-filled solvent trap. Viscosities were measured by monitoring stress as a function of shear rate between 0.01 and 1000 s^{-1}.

Small-Angle X-ray Scattering of Triblock Solutions. Small-angle X-ray scattering experiments were performed on a SAXSLAB Ganesha 300 XL setup with a GeniX-Cu ultralow divergence source with a wavelength of 1.54 $Å^{-1}$ and a flux of 10^8 s^{-1} and a Pilatus 300K silicon pixel detector with 487 × 619 pixels of 172 × 172 $μm^2$. Temperature was controlled between 20 and 60 °C with a Julabo temperature controller. Three detector distances were used, resulting in a q-range of 0.001−2 $Å^{-1}$. Aqueous 292 mg mL^{-1} samples were

DOI: 10.1021/acs.macromol.8b01440
Macromolecules 2018, 51, 8316−8323

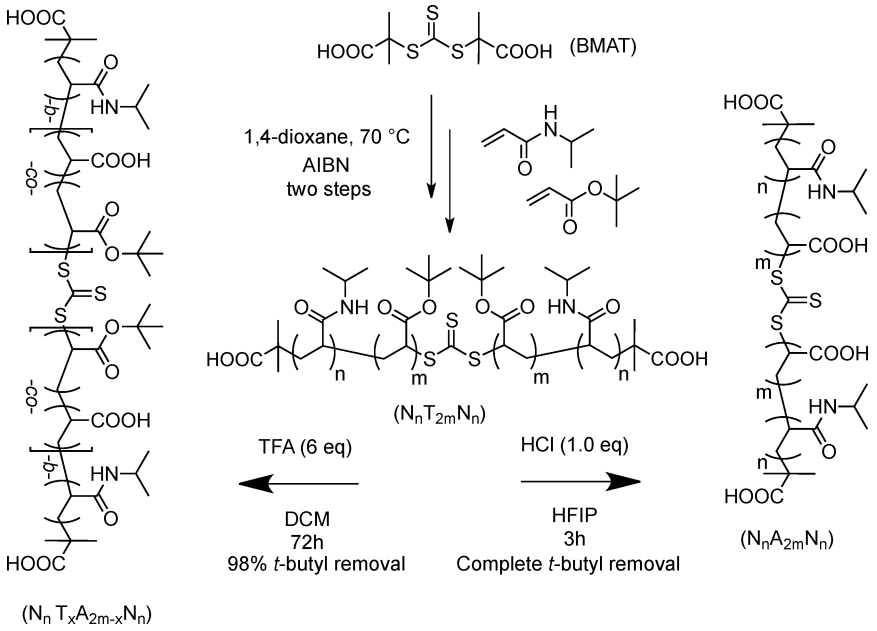

Figure 1. Acidic de-*tert*-butylation of the p*t*BuAc block in an ABA copolymer with pNIPAm using (left) TFA in DCM and (right) dilute stoichiometric HCl in HFIP. Characteristic degrees of *tert*-butoxy group removals are given as percentages.

introduced into 2 mm quartz capillaries, heated to 60 °C, equilibrated for 2 h, and then measured for 1800 s at three different detector distances. This was repeated for 40 and 20 °C. The diffraction patterns were azimuthally averaged, and intensities were corrected for transmission, sample thickness, and detector distance. Finally, scattering from water-filled capillaries corrected in the same fashion was subtracted from the scattering of triblock solutions.

RESULTS AND DISCUSSION

We prepare pNIPAm-*b*-pAA-*b*-pNIPAm (NAN) triblock copolymers from pNIPAm-*b*-*t*BuAc-*b*-pNIPAm (NTN) precursors, as shown in Figure 1 and further detailed in the Supporting Information (Figures S1 and S2). One common *t*Bu-carrying precursor N_{24}-T_{330}-N_{24}, where N_{24} denotes a pNIPAm block length of 24 monomers and T_{330} denotes a p*t*BuAc block length of 330 monomers, serves to compare two acidic ester cleavage reactions: stirring with 6 equiv of TFA in DCM for 72 h and with 1.3 equiv of HCl in HFIP for 4 h. The times are sufficiently long to preclude any further reaction. For TFA/DCM, we choose conditions similar to previous reports on pAA synthesis[12−17] to allow comparison to a situation that is typical in the field.

NMR spectroscopy on aliquots from the reaction mixtures in MeOD shows resonances characteristic of the NIPAm pendant groups at 1.16 and 3.97 ppm, as seen in the NMR spectra of Figure 2a. Contributions of the *t*Bu peak appear at 1.47 and 1.48 ppm, as the dominant peak in NTN precursor, and as a well-noticeable contribution for the TFA-deprotected NAN, even after 72 h. Contrarily, in the HCl-treated case, the residual *t*Bu peak is sufficiently small to be indistinguishable from the tacticity features of the backbone protons, which are well-resolved in MeOD. Save for the resonances attributed to residual *tert*-butyl, the polymeric contributions to the spectra are identical, indicating no other changes to the chemical structure than de-*tert*-butylation.

In Figure 2b, the resonances of backbone and *t*Bu are enlarged, robustly confirming the disappearance of the latter in the case of HCl/HFIP after 3 h. We note that the often-used D_2O does not provide an adequate environment for the *t*Bu

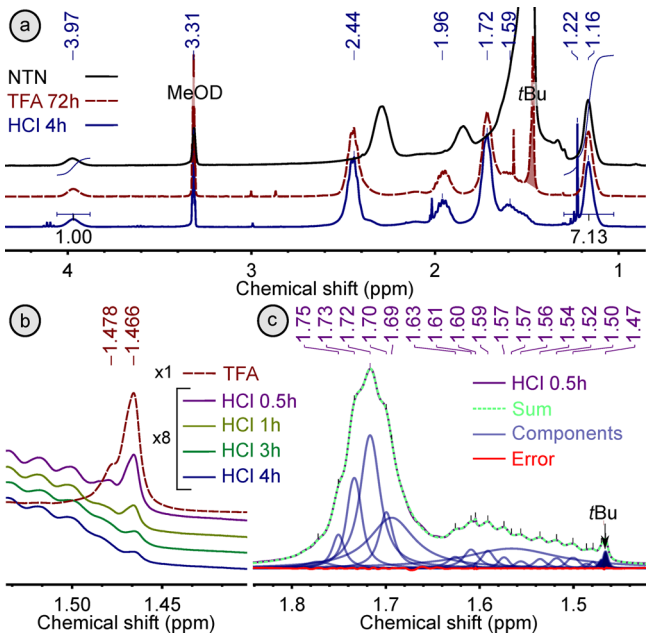

Figure 2. (a) ^{1}H NMR spectra of MeOD solutions of a (top) *t*BuAc copolymer with pNIPAm, (middle) product of deprotection with 6 equiv TFA in DCM, and (bottom) crude sample of deprotection mixture with 1.3 equiv of HCl in HFIP. (b) Enlarged regions of crude samples in MeOD of deprotection with TFA in DCM after 72 h and with HCl in HFIP after 0.5, 1, 3, and 4 h. Note that the HCl/HFIP spectra are inflated 8 times with respect to the TFA/DCM spectrum, after normalization to the pNIPAm methine peak at 3.9 ppm. (c) Deconvolution of a spectrum taken on the deprotection in HCl/HFIP after 0.5 h. The components corresponding to *tert*-butyl protons are filled.

groups to give a sharp signal and thus leads one to underestimate its presence.

Deconvolution of the spectra between 1.4 and 1.8 ppm allows to separate the *t*Bu contribution from the backbone singlets by fitting each peak with a Gaussian−Lorentzian

DOI: 10.1021/acs.macromol.8b01440
Macromolecules 2018, 51, 8316−8323

function. Figure 2c shows a representative case. A comparison of the *N*-isopropylmethine signal at 3.97 ppm to the *t*Bu contribution at 1.47 ppm gives the deprotection efficiency ϕ_D according to

$$\phi_D = 1 - \frac{\frac{1}{9}A_{tBu}}{A_{Nim}}\frac{DP_N}{DP_T} \quad (3)$$

where A_{tBu} and A_{Nim} are the integrals under the deconvoluted *t*Bu contributions and the *N*-isopropylmethine signals, and DP is the degree of polymerization of the block denoted in subscript. This procedure thus provides accurate values for ϕ_D, even in cases where the area under the *t*Bu region is dominated by backbone signals.

Given the improved rate and extent of the reaction, we strongly recommend deprotection with HCl/HFIP above TFA/DCM, with deprotection efficiencies of >99.9% for HCl/HFIP and 90−98% for TFA/DCM. We summarize the deprotection efficiencies ϕ_D of the two methods in Table 1.

Table 1. Molecular Weights and Deprotection Efficiencies of NAN Copolymers[a]

polymer structure	M_{th} (kDa)	M_n (kDa)	$Đ$	treatment	ϕ_D (%)
N_{26}-(A_{312}-T_5)-N_{26}	29.0	14.5	1.47	TFA 6 equiv	98.4
N_{25}-A_{362}-N_{25}	32.5	29.0	1.52	HCl 1.2 equiv	>99.9
N_{36}-A_{220}-N_{36}	24.3	26.8	1.59	HCl 1.0 equiv	>99.9
N_{24}-(A_{297}-T_{33})-N_{24}*	29.5	47.4	1.37	TFA 6 equiv	90.1
N_{24}-A_{330}-N_{24}*	29.2	44.7	1.43	HCl 1.3 equiv	>99.9

[a]Block lengths are based on theoretical molecular weight M_{th} that is based on monomer conversion. M_n and $Đ$ are calculated from SEC traces after elution in 0.01 M aqueous phosphate buffer at pH 7 with 0.1 M $NaNO_3$. Entries marked with an asterisk are used further on in a comparative study of flow behavior, DLS relaxation times, and SAXS.

The entries marked with an asterisk are used for a comparison of flow properties and DLS relaxation times (*vide infra*). As seen in Table 1, HCl/HFIP achieves full *tert*-butyl removal down to 1.0 equiv of HCl. We note that the polymeric contributions to the NMR spectra of all HCl/HFIP-derived products were identical for all acid loadings. Additionally, Table 1 shows deprotection and aqueous SEC characterization data for runs on further NAN structures with slightly varied block lengths. FT-IR data are given in the Supporting Information (Figure S3).

We use aqueous SEC to confirm the triblock identity of our compounds and therefore the stability of the trithiocarbonate bond under conditions of deprotection and subsequent hydrolysis. We find similar values of M_n for both TFA- and HCl-deprotected species, as can be seen in Table 1. Additionally, we intentionally cleaved a sample of N_{24}-A_{330}-N_{24} using hydrazine.[22] Treatment with hydrazine resulted in a discoloration of the sample and a reduction of M_n by a factor of 2, as shown in Figure S4. Thus, the triblocks are quantitatively cleavable, which shows that the trithiocarbonate is stable, even after deprotection and neutralization to pH 7.

We argue that two factors improve the p*t*BuAc de-esterification efficiency of HCl/HFIP with respect to TFA/DCM. DCM is not a solvent for pAA, which prevents contact between the partially deprotected intermediates (essentially pAA/p*t*BuAc copolymers) and the acidic medium. In addition, carboxylates form dimers in apolar environments,[25] further decreasing contact. Our results are not meant to capture the respective contributions of both factors; however, it is clear that TFA/DCM cannot be recommended for the synthesis of highly defined pAA. Because HFIP does not precipitate the product and since HCl is a non-carboxylic acid, both issues are not at play for HCl/HFIP de-*tert*-butylation.

Literature abounds with reports on properties of pAA (co)polymers derived from p*t*BuAc.[14,26] We now turn to the question whether *tert*-butyl moieties influence the solution properties of our copolymers strongly, even when present at the level we found for TFA/DCM. To this end, we studied the difference in the DLS relaxation time and viscosity of aqueous solutions above overlap between triblocks cleaved with TFA and HCl, derived from a common NTN precursor, N_{26}-T_{318}-N_{26}. A common NTN precursor ensures a constant chain length between the two polymers. The NTNs employed in the comparison are labeled with an asterisk in Table 1. In addition, SAXS was used to inquire into structural differences in HCl/HFIP and TFA/DCM products, N_{24}-(A_{297}-T_{33})-N_{24}, where the center block in the latter is the incompletely cleaved p*t*BuAc center block. Additionally, we compared two HCl-deprotected structures of different block lengths, N_{36}-A_{220}-N_{36} and N_{24}-A_{330}-N_{24}.

At a weight concentration of 292 mg mL^{-1} without added salt, all polymers dissolved within 2 days on a shaking bench. Based on an estimate for R_G of 5 nm taken from DLS measurements of dilute solutions at high salt (data not shown), the overlap concentration is below 90 mg mL^{-1} for all triblocks in demineralized water. Thus, our solutions strongly exceed overlap. When heated to 60 °C, which is well above the bulk LCST for pNIPAm homopolymer around 32 °C, both solutions remain transparent. This is in marked contrast to the rapid increase in turbidity that is observed for diblock solutions with a charged block and an LCST block, where the turbidity increase is attributed to formation of micelles due to the association of pNIPAm blocks above the LCST.[14,19,27] In addition to the lack of a turbidty point, we note that our samples show no macroscopic phase separation, in contrast to solutions of pNIPAm homopolymer,[28] copolymers,[29] and derived hydrogels.[30] We remind the reader than pNIPAm and pAA form complexes at a pH far lower than of these samples. Indeed, the solubility of our structures is wholly consistent with the complete deprotonation of pAA at neutral pH.[19]

We note that the mode of association of *t*Bu-free NAN triblocks above overlap is *not* related to micelle formation, as is reported for telechelic polymers with far longer stickers.[31−34] Solutions of HCl-cleaved N_{24}-A_{330}-N_{24} remain transparent even after being heated to 60 °C for 3 days and show a decrease in scattering intensity at 90° when heated to 40 and 60 °C (Figure S5), precluding micellization. Under identical conditions, the TFA-cleaved N_{24}-(A_{297}-T_{33})-N_{24} solutions develop some turbidity and show occasional spikes in scattering intensity. However, SAXS measurements (*vide infra*) again preclude micellization as a cause. DLS measurements on dilute (5 mg mL^{-1}) triblock solutions show no changes in count rate or correlation times upon heating from room temperature to 60 °C, and thus show no evidence of micellization, due to the very short sticker length and high osmotic pressure due to the charged blocks.

DOI: 10.1021/acs.macromol.8b01440
Macromolecules 2018, 51, 8316−8323

When heated from 15 to 60 °C, a 292 mg mL^{-1} solution of N_{24}-A_{330}-N_{24} shows a strong increase in viscosity, whereas none is visually distinguishable for solutions of N_{24}-(A_{297}-T_{33})-N_{24}. This behavior is quantified in Figure 3 (left) by means of

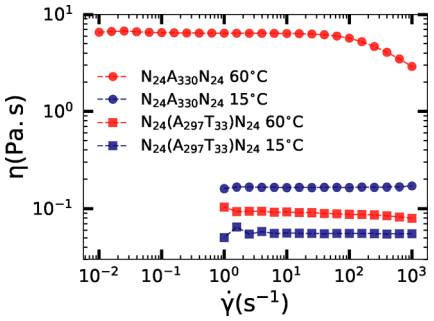

Figure 3. Shear-rate-dependent viscosity of 292 mg mL^{-1} solutions of N_{24}-(A_{297}-T_{33})-N_{24} (squares) and N_{24}-A_{330}-N_{24} (circles) at 15 °C (blue) and 60 °C (red).

rotational rheology in a Couette geometry, where we plot the shear-rate-dependent viscosity for both triblocks, at T above and below the bulk LCST of pNIPAm homopolymer. All viscosity curves are characterized by a wide Newtonian range, and the Newtonian viscosity of the sample increased 70-fold for N_{24}-A_{330}-N_{24}, whereas the increase is marginal for the case of N_{24}-(A_{297}-T_{33})-N_{24}.

We stress that our solutions, upon heating, neither undergo a macroscopic phase transition nor have a cloud point. We merely perceive the effect of the collapse of pNIPAm as the slowed-down relaxation of a transient network. Exactly the unchanged transparency and volume of the samples allowed us to employ DLS to study differences in relaxation times between the two solutions above overlap and below and above the bulk pNIPAm LCST. In Figure 4a, we show averaged first-order normalized correlation functions $g_1(t)$ for both triblocks at 20, 40, and 60 °C. At all temperatures, the correlation functions eventually decay to zero after sufficiently long measurement times (up to 10000 s).

All measured correlation functions are well described by a sum of two stretched exponentials (eq 2), and thus their relaxation is characterized by one slow and one fast mean relaxation time τ_s and τ_f. The fits are plotted as solid lines in Figure 4a, and the relaxation times are plotted against temperature in Figure 4b. A third mode in $g_1(t)$ is also seen, but the acquisition of data of sufficient statistics is prohibitively long for samples at high T, as is clear from Figure 4a. Because its contribution is only minor, it is neglected in the analysis.

The stretch exponents of the fast mode α_f are very close to unity, and the fast modes are exponential. Thus, the fast relaxation times are narrowly distributed. Most of the fast relaxations contribute very little to the overall function, and only in solutions of N_{24}-(A_{297}-T_{33})-N_{24} at 20 °C does the fast mode contribute more than 1% of the signal.

The slow modes exhibit varying degrees of stretching with α_s between 0.76 and 0.95, with α_s increasing with temperature. This suggests that the relaxation rates are more narrowly distributed for transient networks in which the associators have a higher tendency to stick. The dependence of τ_s mirrors the chemistry-dependent thermothickening observed in viscometry. Both the absolute value of τ_s and their temperature variation mode are strongly affected by the chemistry of the middle block. For N_{24}-A_{330}-N_{24}, τ_s is always longer and increases over more than 2 orders of magnitude. Its TFA-cleaved counterpart has a more rapid relaxation of the slow mode and shows only modest growth with temperature.

The three-mode stretched exponential relaxation of $g_1(t)$ in DLS measurements of transient polymer networks has been previously described by other authors,[23,24] where poly(ethylene glycol) networks were formed by association of aliphatic chains, which were attached to the polymers at either one or both ends, yielding "diblock" or "triblock" structures. The relaxation times of the second mode increased strongly with increasing proportion of triblock structures (thus increasing network connectivity) and is ascribed to increased node residence times. Thus, this connectivity increase is analogous to a temperature increase in our experiment. The τ of the third mode is reported to show an even stronger connectivity dependence[23] and is ascribed to diffusion of associated clusters.

Similarly, we attribute the increase of η and τ_s with T to a prolongation of the mean residence time of pNIPAm stickers in the nodes, driven by a higher segregation tendency. The collective effect of the increased residence time is a slowing down of the transient network. The wavevector q is 0.019 nm^{-1}, which means that we are at length scales 1 order of magnitude beyond the node−node correlations. Nonetheless, while τ_s cannot be trivially converted to a residence time, the relaxation time must necessarily increase with residence time.[23] We convey the relaxation of these transient networks in Figure 5—one must realize that the temperature and the extent of deprotection determine the τ over which we would observe relaxation.

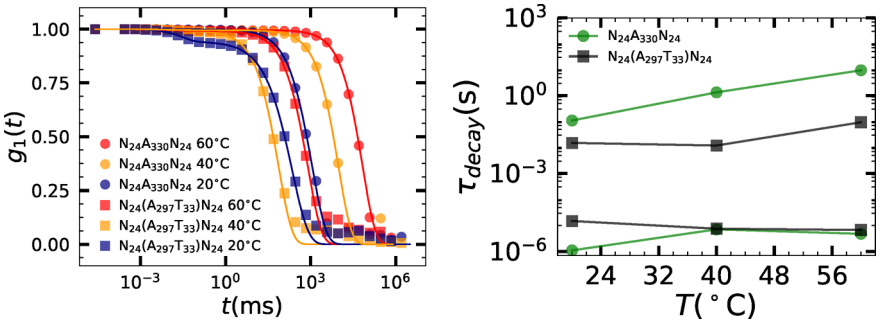

Figure 4. (a) First-order correlation functions from DLS on 292 mg mL^{-1} solutions of N_{24}-A_{330}-N_{24} (squares) and N_{24}-(A_{297}-T_{33})-N_{24} (circles) at 20 °C (blue), 40 °C (orange), and 60 °C (red). The lines are fitted using eq 2. (b) Characteristic slow and fast relaxation times τ_s and τ_f as a function of temperature as fitted using eq 2. The lines are intended as a guide to the eye.

DOI: 10.1021/acs.macromol.8b01440
Macromolecules 2018, 51, 8316−8323

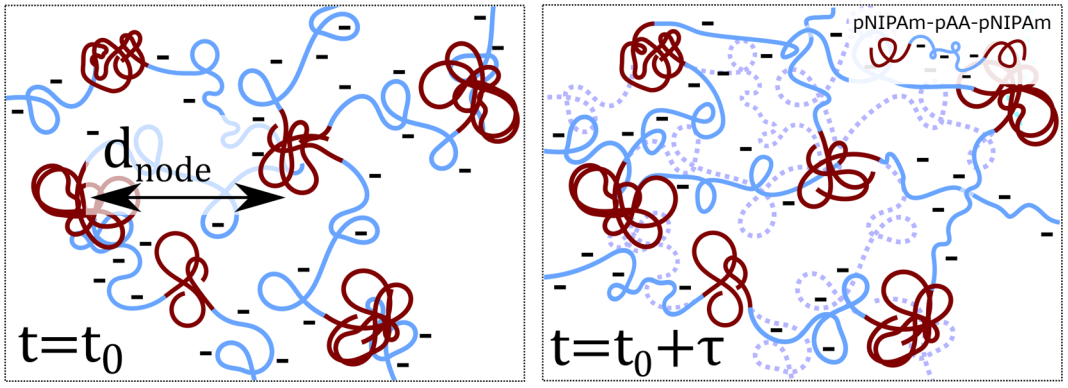

Figure 5. Schematic of two snapshots of a cluster of a few chains in a transient network formed by ABA triblock copolymers. Note that in the range studied temperature and pAA purity do not change the qualitative features of the system: they change only τ, which is the waiting time between the snapshots and is chosen to be above the node residence time and the decorrelation time of the structure on length scales on the order of this box size. The configuration at t_0 is drawn in the rightmost figure as dashed lines. d_{node} is the characteristic internode distance (*vide infra* for its measurement by SAXS). For clarity, the nodes have been portrayed as stationary.

It is remarkable that the availability of hydrophobic groups *decreases* the residence time, since it could be argued that the hydrophobic effect would be stronger with the participation of such groups and thus sticker association more prominent. However, we speculate that the residual esters actually improve compatibility between the pNIPAm and the pAA blocks, which results in *weakening* of the physical cross-links. Additionally, it could be argued that the coils slightly shrink causing them to overlap less. This is consistent with the lower viscosity of the N_{24}-(A_{297}-T_{33})-N_{24} solution at low temperatures and more prominent participation of a fast mode at room temperature.

Additional clues for the origin of short sticker residence times for identical pNIPAm moieties connected to more strongly hydrophobically contaminated pAA come from SAXS, which reveals time-averaged density fluctuations, thus structural information rather than τ-dependent observables. Here, we compare the angle-dependent absolute scattering intensities $\frac{d\Sigma}{d\Omega}(q)$ of 292 mg mL^{-1} solutions of the *tert*-butylated N_{24}-(A_{297}-T_{33})-N_{24} and fully liberated triblocks N_{36}-A_{220}-N_{36} and N_{24}-A_{330}-N_{24} at 20, 40, and 60 °C. All scattering intensities are peaked in the vicinity of $q^* = 0.03$ Å^{-1}, as is visible in Figure 6. The peaks sharpen and shift to smaller q with T, which suggests their origin to be density fluctuations due to increased nonsolubility of pNIPAm with a corresponding internode distance d_{node}. Indeed, a change occurs between 20 and 40 °C, in agreement with an LCST of 32 °C. We attribute the presence of an internode peak below the LCST to pNIPAm−pNIPAm interactions that have been observed in scattering studies of aqueous pNIPAm before,[35] which note a decrease in excluded volume starting already from 5 °C and a consequent clustering below the LCST.[36]

Upon heating from 20 to 60 °C, the internode distance d_{node} that correspond to q^*, at which $\frac{d\Sigma}{d\Omega}$ passes through a prominent maximum, increases from 18.5 to 20.4 nm for N_{36}-A_{220}-N_{36}. Thus, the pAA bridges are stretched to approximately twice their diameter of 10 nm, costing approximately one k_BT assuming entropic elasticity. For N_{24}-A_{330}-N_{24} d_{node} is between 19.3 and 21.9 nm, in line with its longer pAA block. In other regards, the six curves for HCl-derived NAN structures are highly similar, suggesting that the qualitative picture in Figure 5 is correct for all cases and that the chemistry and temperature

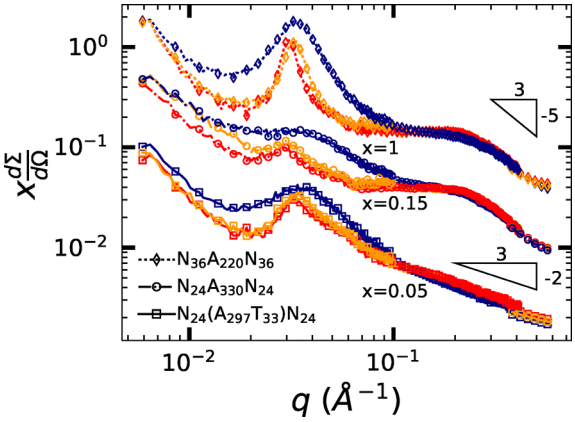

Figure 6. X-ray scattering intensity as a function of modulus of scattering vector q for 292 mg mL^{-1} solutions of one TFA-deprotected and two HCl-deprotected NAN triblock copolymers at 20, 40, and 60 °C in respectively blue, orange, and red (from top to bottom, since the scattering decreases slightly with T). The labels $x = n$ give the scaling factor for the curves, used for better readability. The lines are plotted from the full data, while the marks are plotted only every sixth point.

merely cause changes in the internode distance and sticker residence time of the transient network.

The TFA-deprotected N_{24}-(A_{297}-T_{33})-N_{24} shows smaller values of d_{node}, between 17.6 and 19.7 nm, corresponding to a lesser stretching of the polyelectrolyte block due to more compatibility with the pNIPAm moieties. A striking feature of the curves is the high-q region, where all curves show power laws of, in the case of N_{24}-(A_{297}-T_{33})-N_{24}, $q^{-2/3}$, and, in the case of fully liberated samples, $q^{-5/3}$, the latter corresponding to a self-avoiding walk.[37] We observe these forms up to a d of 1.5 nm, and starting from 5.4 nm for TFA and around 2 nm for the HCl-derived samples, where scattering is dominated by chain statistics ($R_g > d > l_k$).

At present, we have no interpretation of the $q^{-2/3}$ scaling for the TFA-treated case. Clearly, it is not reasonable to attribute it to an even further stretching of the chains than we would expect for a rod (q^{-1}). Thus, the observed shape is likely due to a superposition of different dependencies in the high-q scattering. Nonetheless, we stress that the high-q data witness that TFA leaves us with pAA blocks that have strongly altered

DOI: 10.1021/acs.macromol.8b01440
Macromolecules 2018, 51, 8316−8323

conformational properties with respect to pure pAA blocks. Whereas the structure on the internode length scale is only weakly dependent on temperature and chemistry, the density fluctuations on the chain length scale are strongly altered by *tert*-butyl moieties incompletely cleaved by TFA.

Through DLS, rheology, and visual observations of NAN triblocks around RT and at 60 °C, we observe a significant enhancement of sticker residence times of pNIPAm blocks when the *tert*-butyl group is removed completely, whereas association seems to be minimal when hydrophobic groups have presence. SAXS reveals internode distances of around twice the dilute coil diameter that increase slightly with pAA chain length and absence of hydrophobic groups. More strikingly, the density fluctuations on the chain length scales are dramatically different in the case when *tert*-butyl groups are not completely removed. Thus, the presence of these groups has a strong effect on the self-assembly behavior of NAN copolymers, which are prepared throughout literature through a method that we show does *not* remove *tert*-butyl up to an extent that their influence is negligible.

CONCLUSION

In summary, we report a facile, rapid de-*tert*-butylation scheme for the synthesis of pAA block copolymers with pNIPAm from the corresponding copolymer with p*t*BuAc. The action of stoichiometric HCl on a HFIP solution of the *tert*-butylated precursor yields pAA blocks of a chemical purity that has been inaccessible via the commonly used TFA/DCM mixture. In addition, we show that the presence of residual *tert*-butyl moieties, at a degree tolerated by the latter method, impacts the aqueous self-assembly properties of these polymers to such an extent that the thermothickening effect due to LCST-driven pNIPAm association is essentially disabled for polymer solutions significantly above overlap. Thus, HCl/HFIP is an essential tool in the study of the aqueous association of pAA copolymers derived from their *tert*-butylated precursors.

ASSOCIATED CONTENT

Supporting Information

The Supporting Information is available free of charge on the ACS Publications website at DOI: 10.1021/acs.macromol.8b01440.

Table S1, Figures S1−S4: detailed chemical polymer characterization; Figure S5: light scattering intensities of polymer solutions (PDF)

AUTHOR INFORMATION

Corresponding Author

*Phone + 31 50 363 7888; e-mail marleen.kamperman@rug.nl (M.K.).

ORCID

Alexei D. Filippov: 0000-0002-6492-6238

Ilja K. Voets: 0000-0003-3543-4821

Notes

The authors declare no competing financial interest.

ACKNOWLEDGMENTS

This work was financially supported by the Dutch Science Foundation (NWO VIDI Grant 723.013.005). I.K.V. thanks the Dutch Science Foundation (NWO ECHO Grant No. 712.016.002, NWO VIDI Grant 723.014.006) for financial support. The authors thank Jasper van der Gucht, Thomas Kodger, and Dmitri Filippov for their useful comments.

REFERENCES

(1) Lue, S. J.; Chen, C.-H.; Shih, C.-M. Tuning of Lower Critical Solution Temperature (LCST) of Poly(N-Isopropylacrylamide-co-Acrylic acid) Hydrogels. *J. Macromol. Sci., Part B: Phys.* **2011**, *50* (3), 563−579.

(2) Yoo, M. K.; Sung, Y. K.; Lee, Y. M.; Cho, C. S. Effect of polyelectrolyte on the lower critical solution temperature of poly(N-isopropyl acrylamide) in the poly(NIPAAm-co-acrylic acid) hydrogel. *Polymer* **2000**, *41* (15), 5713−5719.

(3) Bokias, G.; Staikos, G.; Iliopoulos, I. Solution properties and phase behaviour of copolymers of acrylic acid with N-isopropylacrylamide: The importance of the intrachain hydrogen bonding. *Polymer* **2000**, *41* (20), 7399−7405.

(4) Blocher, W. C.; Perry, S. L. Complex coacervate-based materials for biomedicine. *WIREs Nanomed. Nanobiotechnol.* **2017**, *9* (4), e1442.

(5) Liu, Y.; Winter, H. H.; Perry, S. L. Linear viscoelasticity of complex coacervates. *Adv. Colloid Interface Sci.* **2017**, *239*, 46−60.

(6) Loiseau, J.; Doërr, N.; Suau, J. M.; Egraz, J. B.; Llauro, M. F.; Ladavière, C.; Claverie, J. Synthesis and Characterization of Poly(acrylic acid) Produced by RAFT Polymerization. Application as a Very Efficient Dispersant of $CaCO_3$, Kaolin, and TiO_2. *Macromolecules* **2003**, *36*, 3066−3077.

(7) Lena, J.-b.; Goroncy, A. K.; Thevarajah, J. J.; Maniego, A. R.; Russell, G. T.; Castignolles, P.; Gaborieau, M. Effect of transfer agent, temperature and initial monomer concentration on branching in poly (acrylic acid): A study by spectroscopy and capillary electrophoresis. *Polymer* **2017**, *114*, 209−220.

(8) Llauro, M.-F.; Loiseau, J.; Boisson, F.; Delolme, F.; Ladaviere, C.; Claverie, J. Unexpected End-Groups of Poly(acrylic Acid) Prepared by RAFT polymerization. *J. Polym. Sci., Part A: Polym. Chem.* **2004**, *42*, 5439−5462.

(9) Maniego, A. R.; Ang, D.; Guillaneuf, Y.; Lefay, C.; Gigmes, D.; Aldrich-Wright, J. R.; Gaborieau, M.; Castignolles, P. Separation of poly(acrylic acid) salts according to topology using capillary electrophoresis in the critical conditions. *Anal. Bioanal. Chem.* **2013**, *405*, 9009−9020.

(10) Pelet, J. M.; Putnam, D. Poly(acrylic acid) undergoes partial esterification during RAFT synthesis in methanol and interchain disulfide bridging upon NaOH treatment. *Macromol. Chem. Phys.* **2012**, *213* (23), 2536−2540.

(11) Chaduc, I.; Boyron, O.; Charleux, B.; D'Agosto, F.; Lansalot, M. Effect of the pH on the RAFT Polymerization of Acrylic Acid in Water. Application to the Synthesis of Poly(acrylic acid)-Stabilized Polystyrene Particles by RAFT Emulsion Polymerization. *Macromolecules* **2013**, *46*, 6013−6023.

(12) Dulong, V.; Souguir, Z.; Pottier, C.; Picton, L.; Le Cerf, D. Thermo- and pH-Sensitive Triblock Copolymers with Tunable Hydrophilic/Hydrophobic Properties. *J. Polym. Sci., Part A: Polym. Chem.* **2015**, *53*, 2606−2616.

(13) Yong, P.; Yang, Y.; Wang, Z.; Yang, L.; Chen, J. Diverse nanostructures and gel behaviours contained in a thermo- and dual-pH-sensitive ABC (PNIPAM-PAA-P4VP) terpolymer in an aqueous solution. *RSC Adv.* **2016**, *6*, 88306−88314.

(14) Chen, P.; Chen, J.; Cao, Y. Self-assembly behavior of thermo- and Ph-responsive diblock copolymer of poly(N -isopropylacrylamide)- block -poly(acrylic acid) synthesized via reversible addition-fragmentation chain transfer polymerization. *J. Macromol. Sci., Part A: Pure Appl. Chem.* **2013**, *50* (5), 478−486.

(15) Li, G.; Shi, L.; An, Y.; Zhang, W.; Ma, R. Double-responsive core-shell-corona micelles from self-assembly of diblock copolymer of poly(*t*-butyl acrylate-co-acrylic acid)-*b*-poly(N-isopropylacrylamide). *Polymer* **2006**, *47* (13), 4581−4587.

(16) Li, G.; Song, S. E. N.; Guo, L. E. I.; Ma, S. Self-Assembly of Thermo- and pH-Responsive Poly (acrylic acid)-*b*-poly(N-isopropy-

DOI: 10.1021/acs.macromol.8b01440
Macromolecules 2018, 51, 8316−8323

lacrylamide) Micelles for Drug Delivery. *J. Polym. Sci., Part A: Polym. Chem.* **2008**, *46*, 5028−5035.
(17) Lauber, L.; Nicolai, T.; Chassenieux, C.; Colombani, O. Viscoelastic Properties of Hydrogels Based on Self-Assembled Multisticker Polymers Grafted with pH-Responsive Grafts. *Macromolecules* **2017**, *50*, 8178−8184.
(18) Palladino, P.; Stetsenko, D. A. New TFA-free cleavage and final deprotection in Fmoc solid-phase peptide synthesis: Dilute HCl in fluoro alcohol. *Org. Lett.* **2012**, *14* (24), 6346−6349.
(19) Schilli, C. M.; Zhang, M.; Rizzardo, E.; Thang, S. H.; Chong, Y.; Edwards, K.; Karlsson, G.; Müller, A. H. A New Double-Responsive Block Copolymer Synthesized via RAFT Polymerization: Poly (N-isopropylacrylamide)-block-poly (acrylic acid). *Macromolecules* **2004**, *37* (21), 7861−7866.
(20) Lai, J. T.; Filla, D.; Shea, R. Functional polymers from novel carboxyl-terminated trithiocarbonates as highly efficient RAFT agents. *Macromolecules* **2002**, *35*, 6754−6756.
(21) Cetintas, M.; de Grooth, J.; Hofman, A. H.; van der Kooij, H. M.; Loos, K.; de Vos, W. M.; Kamperman, M. Free-standing thermoresponsive nanoporous membranes from high molecular weight PS-PNIPAM block copolymers synthesized via RAFT polymerization. *Polym. Chem.* **2017**, *8* (14), 2235−2243.
(22) Shen, W.; Qiu, Q.; Wang, Y.; Miao, M.; Li, B.; Zhang, T.; Cao, A.; An, Z. Hydrazine as a nucleophile and antioxidant for fast aminolysis of RAFT polymers in air. *Macromol. Rapid Commun.* **2010**, *31* (16), 1444−1448.
(23) Bohdan, M.; Sprakel, J.; Van Der Gucht, J. Multiple relaxation modes in associative polymer networks with varying connectivity. *Phys. Rev. E: Stat. Phys., Plasmas, Fluids, Relat. Interdiscip. Top.* **2016**, *94* (3), 1−7.
(24) Thuresson, K.; Nilsson, S.; Kjøniksen, A.-L.; Walderhaug, H.; Lindman, B.; Nyström, B. Dynamics and Rheology in Aqueous Solutions of Associating Diblock and Triblock Copolymers of the Same Type. *J. Phys. Chem. B* **1999**, *103* (9), 1425−1436.
(25) Fujii, Y.; Yamada, H.; Mizuta, M. Self-association of acetic acid in some organic solvents. *J. Phys. Chem.* **1988**, *92* (23), 6768−6772.
(26) Maniego, A. R.; Sutton, A. T.; Gaborieau, M.; Castignolles, P. Assessment of the Branching Quantification in Poly(acrylic acid): Is It as Easy as It Seems? *Macromolecules* **2017**, *50* (22), 9032−9041.
(27) Bayati, S.; Zhu, K.; Trinh, L. T. T.; Kjøniksen, A. L.; Nyström, B. Effects of temperature and salt addition on the association behavior of charged amphiphilic diblock copolymers in aqueous solution. *J. Phys. Chem. B* **2012**, *116* (36), 11386−11395.
(28) Heskins, M.; Guillet, J. E. Solution Properties of Poly(N-isopropylacrylamide). *J. Macromol. Sci., Chem.* **1968**, *2*, 1441−1455.
(29) Teodorescu, M.; Negru, I.; Stanescu, P. O.; Drăghici, C.; Lungu, A.; Sârbu, A. Thermogelation properties of poly(N-isopropylacrylamide)-*block*-poly(ethylene glycol)-*block*-poly(N-isopropylacrylamide) triblock copolymer aqueous solutions. *React. Funct. Polym.* **2010**, *70* (10), 790−797.
(30) Gan, T.; Guan, Y.; Zhang, Y. Thermogelable PNIPAM microgel dispersion as 3D cell scaffold: effect of syneresis. *J. Mater. Chem.* **2010**, *20* (28), 5937.
(31) De Graaf, A. J.; Boere, K. W. M.; Kemmink, J.; Fokkink, R. G.; Van Nostrum, C. F.; Rijkers, D. T. S.; Van Der Gucht, J.; Wienk, H.; Baldus, M.; Mastrobattista, E.; Vermonden, T.; Hennink, W. E. Looped structure of flowerlike micelles revealed by 1H NMR relaxometry and light scattering. *Langmuir* **2011**, *27* (16), 9843−9848.
(32) McCormick, C. L.; Sumerlin, B. S.; Lokitz, B. S.; Stempka, J. E. RAFT-synthesized diblock and triblock copolymers: thermally-induced supramolecular assembly in aqueous media. *Soft Matter* **2008**, *4* (9), 1760.
(33) Kirkland, S. E.; Hensarling, R. M.; McConaughy, S. D.; Guo, Y.; Jarrett, W. L.; McCormick, C. L. Thermoreversible hydrogels from RAFT-synthesized BAB triblock copolymers: Steps toward biomimetic matrices for tissue regeneration. *Biomacromolecules* **2008**, *9* (2), 481−486.
(34) Lin, Z.; Cao, S.; Chen, X.; Wu, W.; Li, J. Thermoresponsive hydrogels from phosphorylated ABA triblock copolymers: A potential scaffold for bone tissue engineering. *Biomacromolecules* **2013**, *14* (7), 2206−2214.
(35) Lang, X.; Lenart, W. R.; Sun, J. E.; Hammouda, B.; Hore, M. J. Interaction and Conformation of Aqueous Poly(N-isopropylacrylamide) (PNIPAM) Star Polymers below the LCST. *Macromolecules* **2017**, *50* (5), 2145−2154.
(36) Kawaguchi, T.; Kobayashi, K.; Osa, M.; Yoshizaki, T. Is a cloud-point curve in aqueous poly(N-isopropylacrylamide) solution binodal? *J. Phys. Chem. B* **2009**, *113* (16), 5440−5447.
(37) De Gennes, P.-G. *Scaling Concepts in Polymer Physics*; Cornell University Press: Ithaca, NY, 1979.

DOI: 10.1021/acs.macromol.8b01440
Macromolecules 2018, 51, 8316−8323